Journal of Interfaces, Thin films, and Low dimensional systems 6 (1) Summer and Autumn (2022) 559-571

The efficacy of temperature changes and single carbon atom impurity on the thermoelectric properties of the (6, 0) two sided-closed single-walled boron nitride nanotube ((6, 0) TSC-SWBNNTs)

Scientific research paper

Ali Mohammad Yadollahi[1,2*], Mohammad Reza Niazian[1], Masoumeh Firouzi[3], Abolfazl Khodadadi[4]

[1]*Department of Physics, Ayatollah Amoli Branch, Islamic Azad University, Amol, Iran*

[2]*Department of Physics, Takestan Branch, Islamic Azad University, Takestan, Iran*

[3]*Department of Physics, Kashan Branch, Islamic Azad University, Kashan, Iran*

[4]*Department of Physics, North Tehran Branch, Islamic Azad University, Tehran, Iran*

ARTICLE INFO

Article history:
Received 13 February 2023
Revised 2 April 2023
Accepted 6 May 2023
Available online 23 June 2023

Keywords
Coefficient of merit
Nanotube
Electrical conductivity
Seebeck coefficient
Thermal conductivity

ABSTRACT

The present study aims to investigate the thermoelectric properties of a two-sided-closed single-walled boron nitride nanotube (TSC-SWBNNT) with chirality (6, 0). This research has been conducted at different temperatures (200, 300, 500, 700, 900, 1100, and 1300 K) and by injecting the impurity of a single carbon atom instead of nitrogen and boron in different parts of this nanotube. The energy range is from -5.5 eV to +5.5 eV. Based on the obtained results, increasing the temperature and the impurity injection makes the band gap noticeably smaller, with the most decrease at 1300 K. Also, with increasing temperature, the number of peaks decreased, indicating the increased movement of holes and electrons and their decreased localization. As the temperature increases, the height of the thermal conduction peaks increases. However, the thermal conduction values are generally in the range of 10^{-9} nanoscale. The merit of figure (ZT) values increased with the increase of temperature, with the highest values obtained at 1300 K. The high ZT values, especially at high temperatures, indicate that (6, 0) TSC-SWBNNT is appropriate to be chosen as a thermoelectric material.

1 Introduction

Applying a temperature difference between the two ends of a material excites the charge carriers on the hot side of the material by absorbing energy. As a result, it moves them from the hot side of the material to its cold side. As the carriers accumulate in the cold part of the material, the charge neutrality is lost, and an internal electric field is formed to prevent further carrier migration. Finally, the balance is achieved, and an electric voltage difference is created along the material length according to the temperature gradient [1-2].

The coefficient of merit (ZT) is an essential thermoelectric property that depends on thermal and electrical conductivity. High ZT requires low thermal conductivity, high electrical conductivity, and a high Seebeck coefficient [1, 3].

In addition, an increase in temperature causes an increase in ZT. In this respect, the conduction of phonons is different from the conduction of electrons. The mean free path of electrons is only from a few Å to

*Corresponding author.
Email address: a11335533@gmail.com
DOI: 10.22051/jitl.2023.42796.1081

a few nanometers. On the other hand, the mean free path of phonons has a large range from a few nanometers to several hundred micrometers, depending on the crystal structure and microstructure of the material. Therefore, scattering sites with length scales larger than a few nanometers cannot affect electrons much, while they can effectively scatter phonons with comparable mean free paths. Hence, this phenomenon is an effective solution to reduce the thermal conductivity of the lattice and has little effect on electrical conductivity. This method is called nanostructured or small-size thermoelectric [1, 4-8].

Nanotubes are particular types of nanostructures. Since the production of carbon nanotubes by Ijima in 1991, these nanotubes have become the focus of research in various fields regarding their unique tubular structure and excellent properties [9]. Nanotubes always have been of interest in terms of electronic and thermoelectric transport. Carbon nanotubes have unique mechanical, electrical, and thermal properties. Accordingly, they can be used to make transistors and transmission the generated heat [1, 10]. Phonons play a large role in the thermal conductivity of nanotubes. The contribution of phonons to the thermal power of carbon nanotubes is a hundred times higher than the contribution of electrons [1, 11]. Among other types of nanotubes, the boron nitride nanotube has better electrical and thermal properties than the carbon nanotube. Also, the boron nitride nanotube has high biocompatibility.

Boron nitride nanotubes are structurally similar to carbon nanotubes: carbon atoms in a hexagonal plane are alternately replaced by B and N atoms with almost no change in atomic distance. These nanotubes were theoretically predicted in 1994 and synthesized a year later via electric arc discharge [9, 12]. Unlike carbon nanotubes, boron nitride nanotubes are electrical insulators with a band gap of about 5.5-6 eV, independent of the diameter, chirality, and number of nanotube walls [13]. It has also been reported that for zigzag boron nitride nanotubes with a diameter smaller than 1 nm, their band gap is affected by radius changes [14].

Due to the polar nature of the B-N bond, boron nitride nanotubes can form a stronger bond with polymers [15]. Regarding thermal properties, the thermal conductivity of boron nitride nanotubes competes with carbon nanotubes of the same diameter [16]. In addition, boron nitride nanotubes show better thermal stability. The oxidation reaction of carbon nanotubes takes place at 500℃ in air, while boron nitride nanotubes are resistant up to 900℃ under the same conditions [17-18]. The high absorption of neutrons by boron makes boron nitride nanotubes suitable to use in shielding materials against neutron radiation, which can lead to catastrophic failure for human space missions [19-20].

Zigzag and armchair boron nitride nanotubes doped with carbon were investigated in terms of electronic structure and compared with pure boron nitride nanotubes [21]. The results confirmed that carbon substitution with boron and nitrogen in boron nitride nanotubes reduced the conduction energy band gap from 5.1 to 1.3 eV compared to pure boron nitride nanotubes, thereby increasing its electron transport ability. However, there are studies on producing intrinsically doped boron nitride nanotubes without using external effects [22].

The boron nitride nanotube is composed of two elements (i.e., nitrogen and boron). Therefore, the bond between them is partially ionic due to the electronegativity between these two elements. This electronegativity causes a band gap of 5-6 eV for this boron nitride nanotube, which does not depend on its chirality and diameter [1, 13, 23]. Considering the wide applications of boron nitride nanotubes, in this paper, the thermoelectric properties of two sided-closed single-walled boron nitride nanotube (TSC-SWBNNT) with chirality (6, 0) between two electrodes made of (5,5) carbon nanotubes are investigated. The experiments were conducted at different temperatures (200, 300, 500, 700, 900, 1100, and 1300 K) and by injecting the impurity of a single carbon atom instead of nitrogen and boron in different parts of this nanotube. The energy range is from -5.5 eV to +5.5 eV. For this purpose, tight-binding approximation and non-equilibrium Green's function approach (NEGF), Slater-Koster [24-25], and Force Field [24, 26] methods were used. Finally, a reliable ATK software package was used for the simulation [27].

2 Simulation and model

According to Fig. 1, the total number of atoms of nitrogen and boron in the (6, 0) TSC-SWBNNT is 112. According to Fig. 2, the diameter of the (6, 0) TSC-

SWBNNT is about 5.8 Å, and its length is about 19.9 Å. Both sides of the (6, 0) TSC-SWBNNT are closed with boron and nitrogen atoms as pentagonal and hexagonal structures. The (6, 0) TSC-SWBNNT axis is considered parallel to the z-axis.

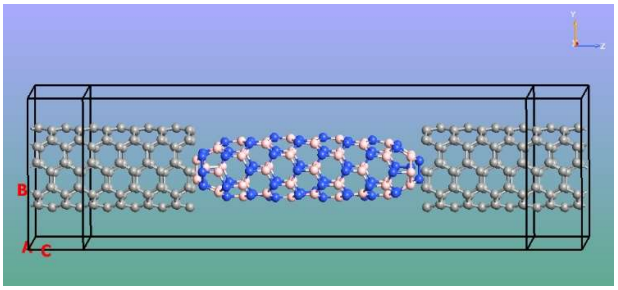

Figure 1. Device made with pure (6, 0) TSC-SWBNNT and two (5, 5) carbon nanotube electrodes on both sides.

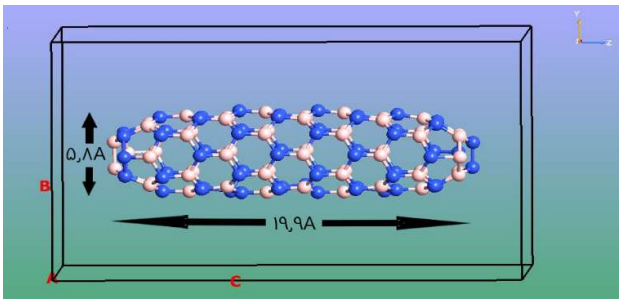

Figure 2. (6, 0) TSC-SWBNNT.

According to Figs. 3a-3f, the carbon atom has replaced boron and nitrogen atoms in parts of the central (Figs. 3a and 3b), left (Figs. 3c and 3d), and right (Figs. 3e and 3f). Because the atom of carbon has one electron more than the atom of boron, by swapping the atom of carbon with the atom of boron, one electron is injected into the (6, 0) TSC-SWBNNT. This impurity can convert (6, 0) TSC-SWBNNT into an n-type semiconductor. Besides, the carbon atom has one electron less than the nitrogen atom. By swapping the carbon atom with the nitrogen atom, a hole is injected into the (6, 0) TSC-SWBNNT, and this impurity can convert the (6, 0) TSC-SWBNNT. 0) into a p-type semiconductor [28-29].

Due to the large number of atoms, suitable simulation software can be used in this case. One of these software packages is Quantum ATk software, which is used in this article. This research employs non-equilibrium Green's function approach and tight-binding approximation, Slater-Koster [25], and Force Field [26] methods. Pentagons and hexagons, which are made of nitrogen and boron atoms, close both sides of this nanotube. The (6, 0) TSC-SWBNNT axis is parallel to the axis of z. The Mesh cut-off is 150 Rydberg [30-31] during the simulation procedure. Brillouin zone was considered with K-point, 1×1×100 [24, 32]. Tolerance of the force of 0.01 eV/A with a maximum step of 500 was

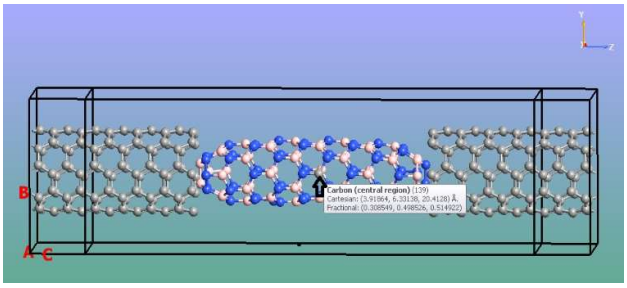

Figure 3a. Device made with (6, 0) TSC-SWBNNT with carbon atom impurity instead of boron atom in the center and two (5, 5) carbon nanotube electrodes on both sides.

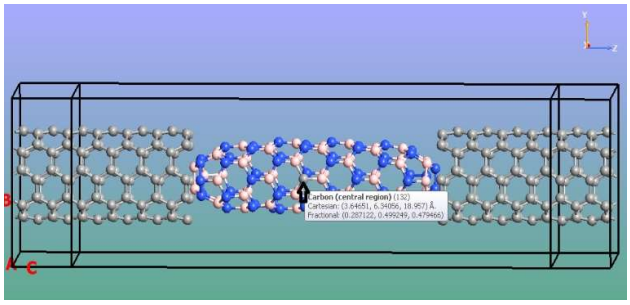

Figure 3b. Device made with (6, 0) TSC-SWBNNT with carbon atom impurity instead of nitrogen atom in the center and two (5, 5) carbon nanotube electrodes on both sides.

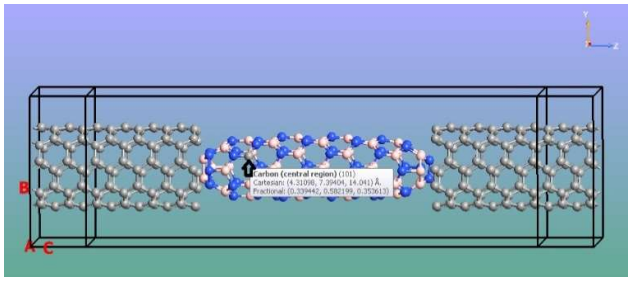

Figure 3c. Device made with (6, 0) TSC-SWBNNT with carbon atom impurity instead of boron atom on the left side and two (5, 5) carbon nanotube electrodes on both sides.

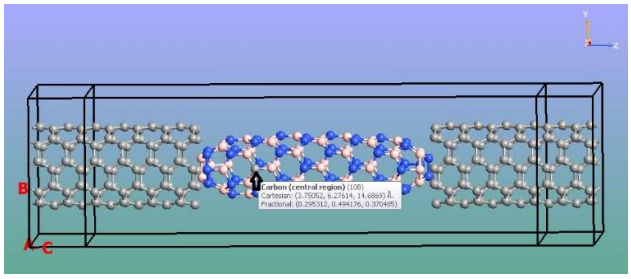

Figure 3d. Device made with (6, 0) TSC-SWBNNT with carbon atom impurity instead of nitrogen atom on the left side and two (5, 5) carbon nanotube electrodes on both sides.

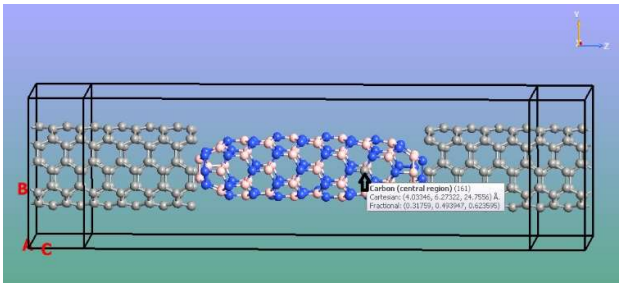

Figure 3e. Device made with (6, 0) TSC-SWBNNT with carbon atom impurity instead of boron atom on the right side and two (5, 5) carbon nanotube electrodes on both sides.

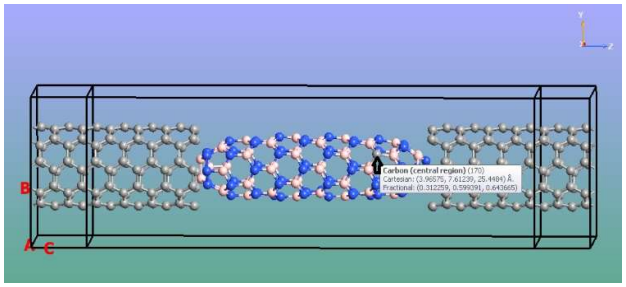

Figure 3f. Device made with (6, 0) TSC-SWBNNT with carbon atom impurity instead of nitrogen atom on the right side and two (5, 5) carbon nanotube electrodes on both sides.

used to optimize the device. In addition, the carbon nanotube (5, 5) with a repetition number of 1×1×4 was used in the electrodes. After making the (6, 0) TSC-SWBNNT device and optimizing and making the mentioned settings, the program was implemented. The function of transmission T (E, V) with bias voltage V and energy E according to NEGF relationships is obtained using the following formula [33-34]:

$$T(E,V) = Tr[\Gamma_L(V)G^R(E,V)\Gamma_R(V)G^A(E,V)], \quad (1)$$

where G^R and G^A are the retarded and advanced Green functions of the central scattering region, respectively. $\Gamma_{LR} = i[\sum_{L(R)}^{R}(E) - \sum_{L(R)}^{A}(E)]$ is broadening function, $\sum_{L(R)}^{R}(E)$ and $\sum_{L(R)}^{A}(E)$ are the self-energies of the central scattering region that include all effects of the electrodes [33-34].

The current of the system is given by the Landauer-Butikker relationship [34-36]:

$$I(V) = \frac{2e}{h}\int [f(E-\mu_L) - f(E-\mu_R)]T(E,V)dE, \quad (2)$$

where h is the Planck's constant, e is the electron charge, $f(E-\mu_{L(R)})$ is a function of the Fermi distribution of electrons in the left (right) electrode, and $\mu_{L(R)}$ is the electrochemical potential of the left (right) electrode [34-36].

In the linear response area, thermoelectric coefficients are obtained by applying a voltage difference (dV) or temperature difference (dT) between two electrodes from the following relations. Electrical conductivity (Ge) is obtained from the following equation [34-36]:

$$G_e = \left.\frac{dI}{dV}\right|_{dT=0}. \quad (3)$$

The Peltier coefficient is obtained from the following relationship [34-36]:

$$\Pi = \left.\frac{I_Q}{I}\right|_{dT=0}. \quad (4)$$

The Seebeck coefficient (thermal capacity) is [34-36]:

$$S = -\left.\frac{dV}{dT}\right|_{I=0} = \frac{\Pi}{V}. \quad (5)$$

The coefficient of thermal conductivity, i.e., the sum of the thermal conductivity coefficient of a phonon and the thermal conductivity coefficient of the electron, is as follows [34-36]:

$$\kappa = \kappa_e + \kappa_{ph} = \left.\frac{dI_Q}{dT}\right|_{I=0}, \quad (6)$$

where the thermal current is obtained from the following relationship [34-36]:

$$I_Q = dQ/dT. \quad (7)$$

Considering the above thermoelectric coefficients, the dimensionless coefficient of merit (ZT), is derived as [34-36]:

$$ZT = \frac{G_e S^2 T}{k}. \quad (8)$$

3 Results and discussion

In this paper, thermoelectric properties of (6, 0) TSC-SWBNNT at different temperatures of 200, 300, 500, 700, 900, 1100, and 1300 K and applying impurity of carbon instead of nitrogen and boron in three states of the right, left and center sides of this nanotube are investigated. Figures 4a-4g illustrate the electrical conductivity (Ω^{-1}) of (6, 0) TSC-SWBNNT in the impurity of carbon states instead of nitrogen and boron. In all figures, the right half of the curves is longer or equal to the left half of the same curve, suggesting the almost equal density of charge carriers in both valence and conduction bands. In all these shapes, the height of the peaks decreased with increasing temperature [1,28]. As a result, these electrons and holes have moved more towards the lowest unoccupied molecular orbital (LUMO) and highest occupied molecular orbital (HOMO) levels, reducing the band gap and increasing the conduction. The number of excited phonons increases as temperature rises, preventing the easier passage of charge carriers and thus reducing electrical conductivity. Also, as the temperature rises, the number of peaks decreases, indicating that the electrons and holes mobility has increased while their localization has decreased. With the increase in temperature, the band gap has also decreased significantly. In this respect, the largest decrease can be seen at the temperature of 1300 K in Figs. 4a-4g. By substituting the carbon atom instead of boron (and because the carbon atom has one electron more than boron) and injecting this extra electron, the nanotube becomes an n-type semiconductor [11, 37-38]. Hence, the band gap from the right side decreases noticeably. Moreover, by substituting the atom of carbon instead of the atom of nitrogen and considering that the atom of carbon has one electron less than the atom of nitrogen, the (6, 0) TSC-SWBNNT turns into a semiconductor of p-type [11,37-38]. As a result, the band gap decreases more from the left side. The greatest decrease in band gap and change in electrical conductivity is related to Figs. 4b and 4c at 1300 K temperature, where the carbon atom is placed in the center instead of boron and nitrogen atoms, respectively [28]. Notably, the effect of this impurity in the center is more visible than the impurities on the right and left sides. This result is attributed to replacing carbon atoms instead of boron and nitrogen atoms and converting the nanotube into n- and p-type semiconductors, respectively, and the higher density of holes and electrons at both ends of the nanotube and near the boundaries.

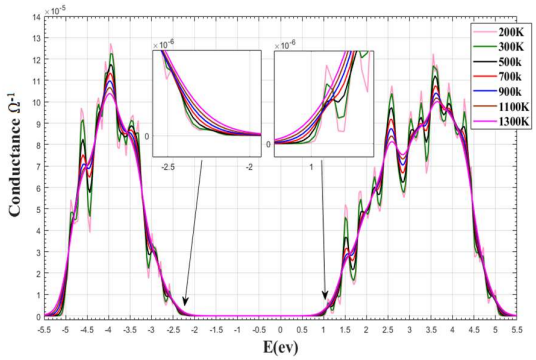

Figure 4a. Electrical conductivity of (6, 0) TSC-SWBNNT without impurities at different temperatures

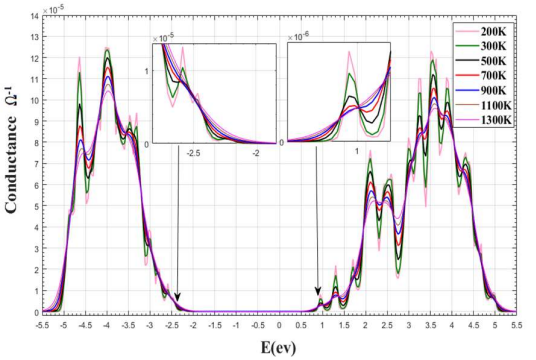

Figure 4b. Electrical conductivity of (6, 0) TSC-SWBNNT with carbon impurity instead of boron in the center at different temperatures

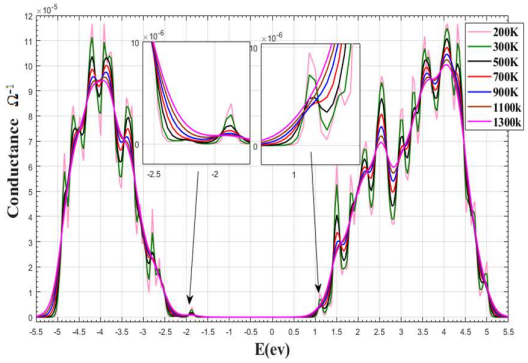

Figure 4c. Electrical conductivity of (6, 0) TSC-SWBNNT with carbon impurity instead of nitrogen in the center at different temperatures

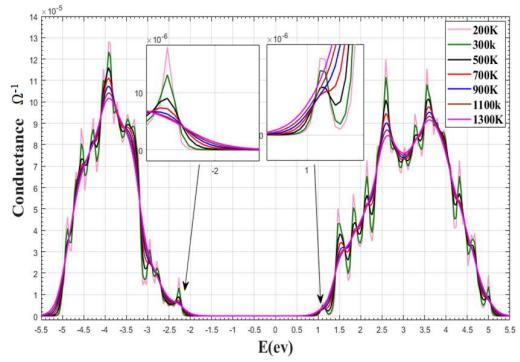

Figure 4d. Electrical conductivity of (6, 0) TSC-SWBNNT with carbon impurity instead of boron on the left side at different temperatures

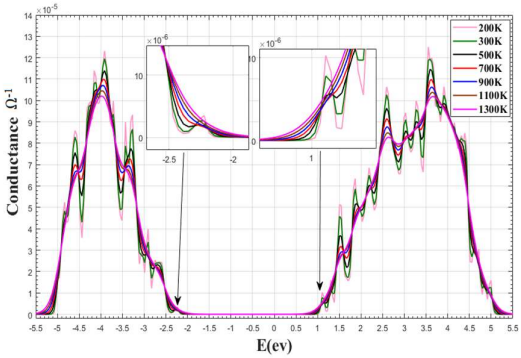

Figure 4e. Electrical conductivity of (6, 0) TSC-SWBNNT with carbon impurity instead of nitrogen on the left side at different temperatures

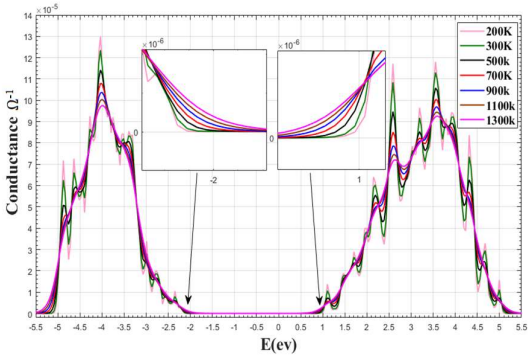

Figure 4f. Electrical conductivity of (6, 0) TSC-SWBNNT with carbon impurity instead of boron on the right side at different temperatures

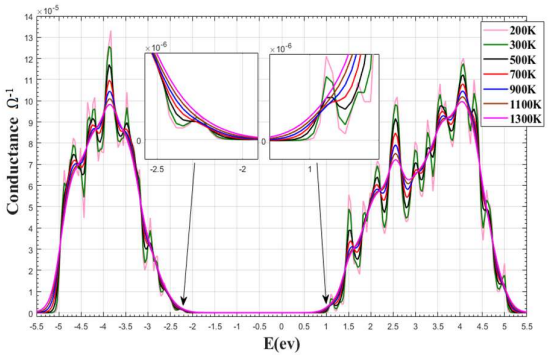

Figure 4g. Electrical conductivity of (6, 0) TSC-SWBNNT with carbon impurity instead of nitrogen on the right side at different temperatures

Figures 5a-5g depict the coefficient of Seebeck for different states of carbon impurity instead of nitrogen and boron in the right, left, and center sides of the (6, 0) TSC-SWBNNT. Figures 5a-5g are related to the coefficient of Seebeck's figure at different temperatures. With the increase in temperature, the peak number in the coefficient of Seebeck has decreased, suggesting that the electrons' mobility and holes increase and their localization decreases. Nevertheless, the most changes in the Seebeck coefficient in these figures are in the band gap range. The peak height increases with increasing temperature, indicating an increase in the coefficient of Seebeck. The maximum peak height corresponds to 1300 K in the range of -0.5 to -1.5 eV (Figs. 5a-5g). Meanwhile, the highest peak height of the coefficient of Seebeck in these figures is related to 1300 K and in the case of carbon impurity instead of nitrogen in the center of the nanotube. The maximum value of the coefficient of Seebeck is about 750 μV/K. In these figures, the lowest value of the Seebeck coefficient is about -950 μV/K, which is related to the impurity of carbon instead of nitrogen on the right side of the (6, 0) TSC-SWBNNT.

Figures 6a-6g display the thermal conductivity of different states of carbon impurity instead of nitrogen and boron in the three parts of the right, left, and center sides of the (6, 0) TSC-SWBNNT. As can be seen, the altitude of the peaks increases as the temperature rises, indicating the increase in thermal conductivity with the temperature increase. In all figures, half of the right of the curves is longer or equal to the left half of the same curve, which shows the charge carriers' density in the valence and conduction bands. However, the thermal

conductivity values are in the range of 9-10 nm, which are small values. According to Eq. (8), as thermal

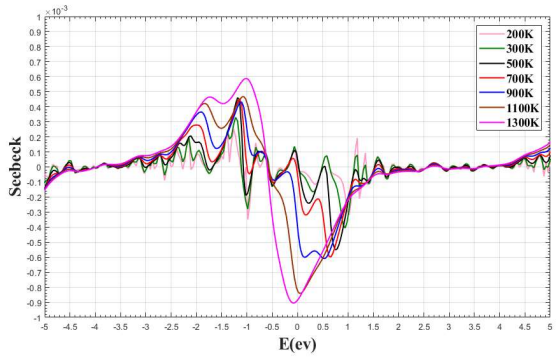

Figure 5a. Seebeck coefficient (thermal power) of (6, 0) TSC-SWBNNT without impurities at different temperatures

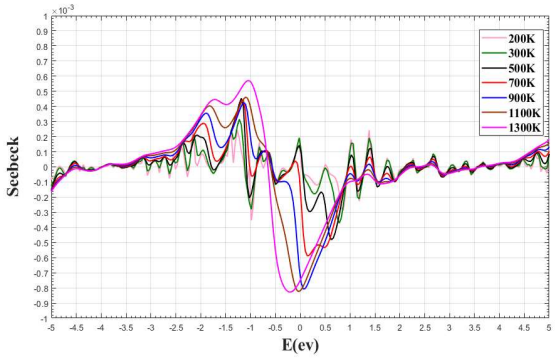

Figure 5b. Seebeck coefficient (thermal power) of (6, 0) TSC-SWBNNT with carbon impurity instead of boron in the center at different temperatures

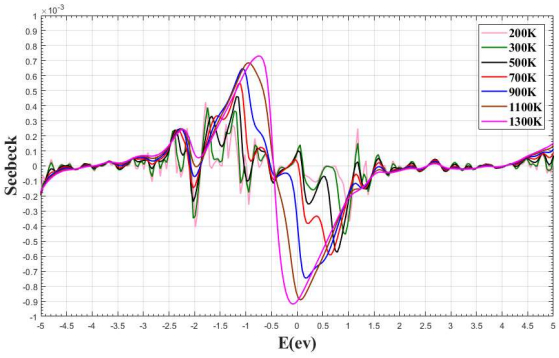

Figure 5c. Seebeck coefficient (thermal power) of (6, 0) TSC-SWBNNT with carbon impurity instead of nitrogen in the center at different temperatures

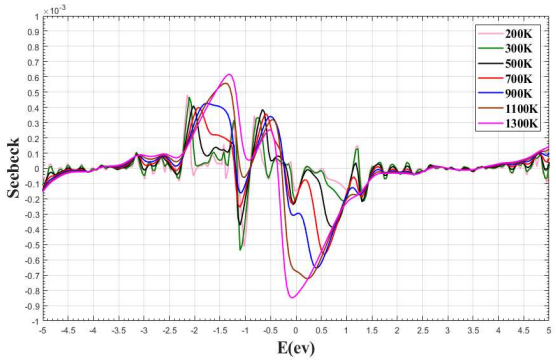

Figure 5d. Seebeck coefficient (thermal power) of (6, 0) TSC-SWBNNT with carbon impurity instead of boron on the left side at different temperatures

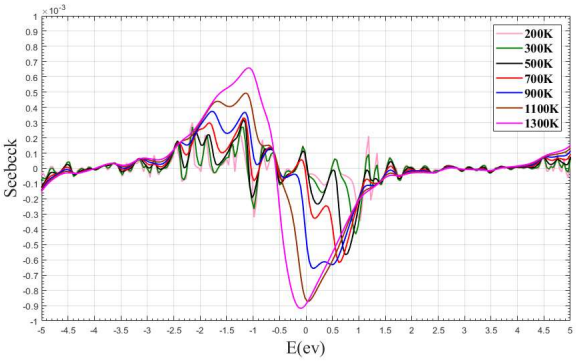

Figure 5e. Seebeck coefficient (thermal power) of (6, 0) TSC-SWBNNT with carbon impurity instead of nitrogen on the left side at different temperatures

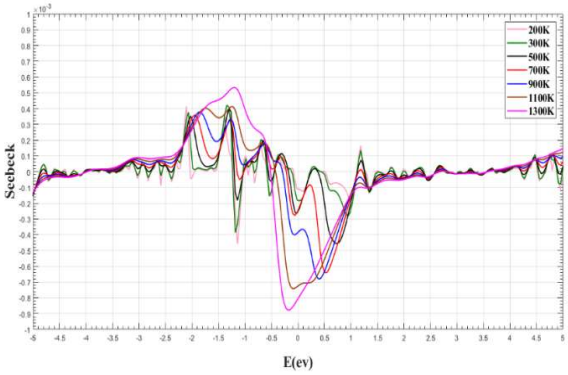

Figure 5f. Seebeck coefficient (thermal power) of (6, 0) TSC-SWBNNT with carbon impurity instead of boron on the right side at different temperatures

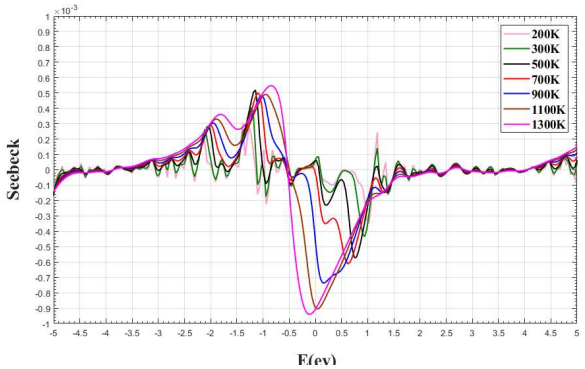

Figure 5g. Seebeck coefficient (thermal power) of (6, 0) TSC-SWBNNT with carbon impurity instead of nitrogen on the right side at different temperatures.

conductivity is in the equation denominator, ZT increases with a decrease in thermal conductivity. Due to the attendance of the phonon, curves in Figs. 6a-6g have been slightly shifted upwards. The highest total thermal conductivity is related to the impurity state of carbon instead of nitrogen in the center (6-c), (6, 0) TSC-SWBNNT, which has a value of 3.3 nW at an energy value of 3.8 eV. K is the lowest of total thermal conductivity at 1300 K, corresponding to the state without impurities (6, 0) TSC-SWBNNT. Moreover, as can be inferred from Figs. 6a-6g, the band gap has decreased noticeably with temperature rise, and the reduction is different based on the semiconductor type in terms of carbon impurity instead of nitrogen (p) or boron (n).

The ZT values for the (6, 0) TSC-SWBNNT are shown in Figs. 7a-7g. These figures were drawn based on the impurity of carbon atoms instead of nitrogen and boron atoms in the right, left, and central the (6, 0) TSC-SWBNNT. These figures exhibit the ZT change in terms of temperature (K) change. With the increase in temperature, the ZT values increased in all figures, with the highest values related to 1300 K. With the increase in temperature, the number of peaks decreased. This result is caused by the greater mobility of electrons and holes with the increase in temperature and their less localization. Furthermore, with increasing temperature, the length of the band gap has also decreased. The highest ZT is related to the impurity state of a carbon atom instead of a boron atom in the center of the (6, 0) TSC-SWBNNT at 1300 K (Fig. 7b), which is 2.25 at an energy of -5.2 eV. Considering the high values of ZT, especially at high temperatures, the (6, 0) TSC-SWBNNT seems suitable to choose as a thermoelectric material.

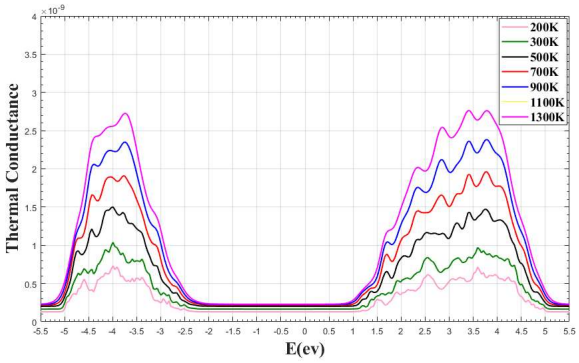

Figure 6a. Thermal conductivity of (٦ ,٠)TSC-SWBNNT without impurities at different temperatures.

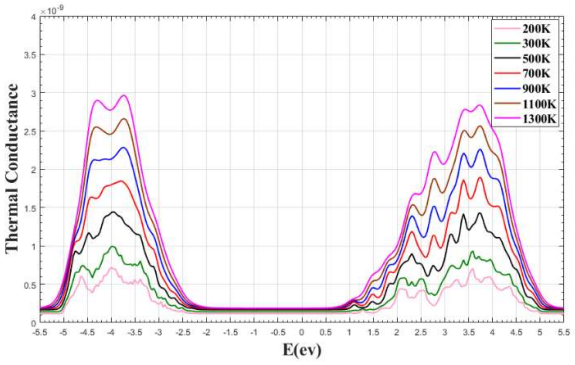

Figure 6b. Thermal conductivity of (٦ ,٠)TSC-SWBNNT with carbon impurity instead of boron in the center at different temperatures.

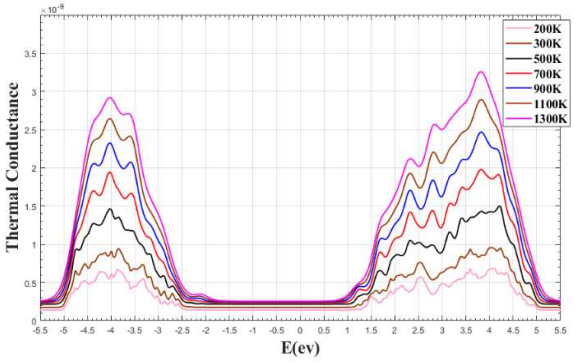

Figure 6c. Thermal conductivity of (٦ ,٠)TSC-SWBNNT with carbon impurity instead of nitrogen in the center at different temperatures.

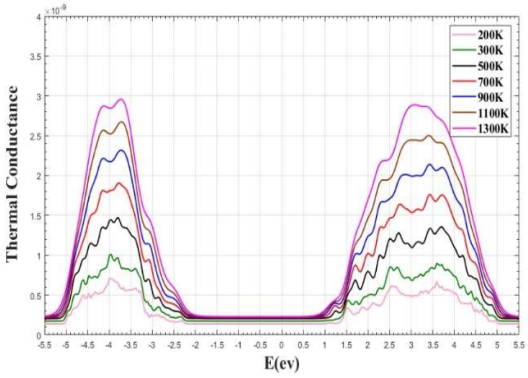

Figure 6d. Thermal conductivity of (۰ ,۲)TSC-SWBNNT with carbon impurity instead of boron on the left side at different temperatures.

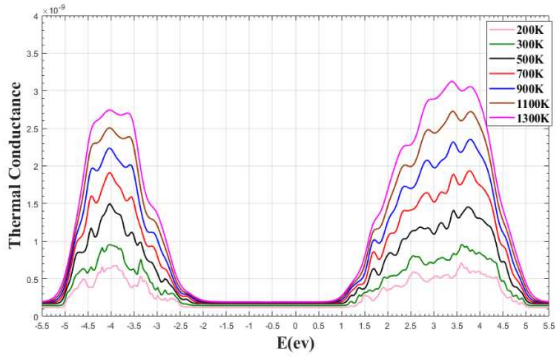

Figure 6e. Thermal conductivity of (6, 0) TSC-SWBNNT with carbon impurity instead of nitrogen on the left side at different temperatures.

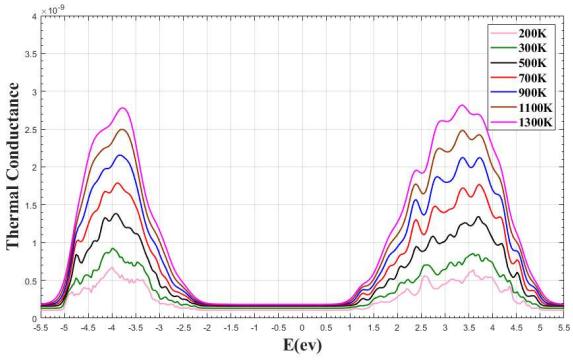

Figure 6f. Thermal conductivity of (6, 0) TSC-SWBNNT with carbon impurity instead of boron on the right side at different temperatures.

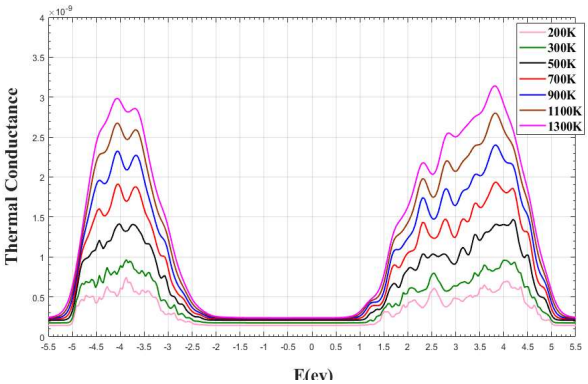

Figure 6g. Thermal conductivity of (6, 0) TSC-SWBNNT with carbon impurity instead of nitrogen on the right side at different temperatures.

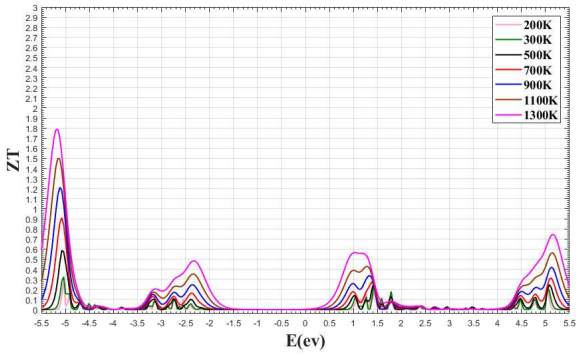

Figure 7a. Merit coefficient (ZT) of (6, 0) TSC-SWBNNT without impurity at different temperatures.

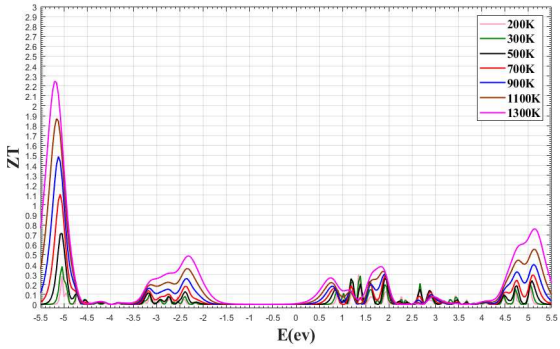

Figure 7b. Merit coefficient (ZT) of (6, 0) TSC-SWBNNT with carbon impurity instead of boron in the center at different temperatures.

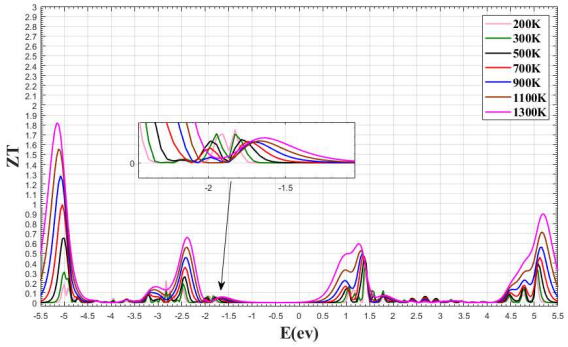

Figure 7c. Merit coefficient (ZT) of (6, 0) TSC-SWBNNT with carbon impurity instead of nitrogen in the center at different temperatures.

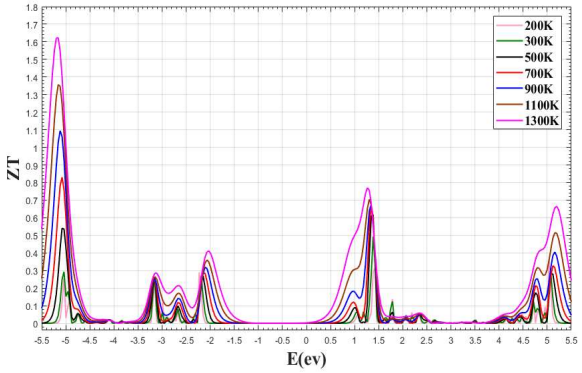

Figure 7d. Merit coefficient (ZT) of (6, 0) TSC-SWBNNT with carbon impurity instead of boron on the left side at different temperatures.

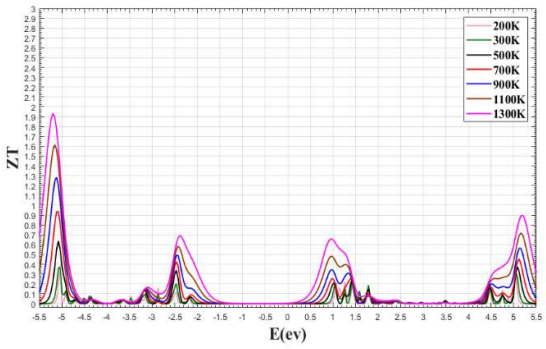

Figure 7e. Merit coefficient (ZT) of (6, 0) TSC-SWBNNT with carbon impurity instead of nitrogen on the left side at different temperatures.

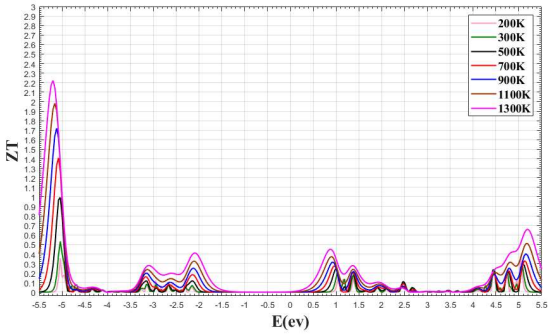

Figure 7f. Merit coefficient (ZT) of (6, 0) TSC-SWBNNT with carbon impurity instead of boron on the right side at different temperatures.

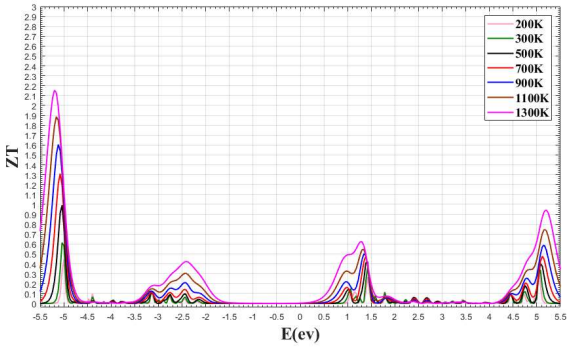

Figure 7g. Merit coefficient (ZT) of (6, 0) TSC-SWBNNT with carbon impurity instead of nitrogen on the right side at different temperatures.

4 Conclusions

In this research, the thermoelectric characteristics of (6, 0) TSC-SWBNNT are investigated in the state without impurity and single carbon atom impurity instead of nitrogen and boron atoms in the right, left, and center side of this nanotube. The study is conducted in the energy range of -5.5 to 5.5 eV and in temperatures of 200, 300, 500, 700, 900, 1100 and 1300 K. The overall results of this article are as follows:

1- In all thermal power (Seebeck coefficient) figures, the number of peaks has decreased with increasing temperature, indicating that the mobility of holes and electrons grows and their localization decreases. However, the most changes in thermal power in these figures are in the band gap range. As temperature increases, the height of the peaks increases, suggesting an increase in thermal power.

2- The highest amount of thermal power in the thermal power figures is related to the carbon atom impurity instead of nitrogen in the center, which occurs at 1300 K.
3- As can be seen from the thermal conductivity figures, the altitude of the peaks increases with increasing temperature, indicating the increase in thermal conductivity with increasing temperature. Nevertheless, the values of thermal conductivity are generally in the range of 9-10 nm, which are small values. According to Eq. (8), as thermal conductivity is in the equation denominator, ZT increases with a decrease in thermal conductivity. Due to the presence of phonon, the curves slightly shifted upward.
4- According to the thermal conductivity figures, the band gap has significantly decreased with the increase in temperature. Besides, the amount of reduction is different based on the type of semiconductor in terms of the impurity of carbon instead of nitrogen (p) and boron (n).
5- With the increase of temperature in the figures related to ZT, the ZT values increased, with the highest values corresponding to 1300 K. As temperature rises, the number of peaks decreases. This result is due to the greater mobility of electrons and holes with the increase in temperature and their less localization. Also, as temperature increases, the length of the band gap also decreases.
6- Regarding the high values of 1 for ZT, especially at high temperatures, the (6, 0) TSC-SWBNNT seems suitable to choose as a thermoelectric material.

References

[1] A. M. Yadollahi et al., "Effect of temperature changes on thermoelectric properties of the two sided-closed single-walled BNNTs (6, 3)." Journal of Interfaces, Thin Films, and Low dimensional systems (JITL), **5** (2022) 421.

[2] S. LeBlanc, "Thermoelectric generators: Linking material properties and systems engineering for waste heat recovery applications." Sustainable Materials and Technologies, **1** (2014) 26-35.

[3] G. J. Snyder, E.S. Toberer, "Complex thermoelectric materials." Nature materials, **7** (2008) 105.

[4] M. Yaghobi et al., "Electronic transport through a C_{60-n} X_n(X^N and B) molecular bridge." Molecular Physics, **109** (2011) 1821.

[5] C. Joachim et al., "Analysis of low-voltage I (V) characteristics of a single cgo molecule." Europhys. Letters, **30** (1995) 409.

[6] Moh. Yaghobi et al., "Magnetic and structural properties of BNC nanotubes." Molecular Physics, **117** (2019) 260.

[7] A. Minnich et al., "Bulk nanostructured thermoelectric materials: current research and future prospects." Energy & Environmental Science, **2** (2009) 466.

[8] M. Weber et al., "Novel and Facile Route for the Synthesis of Tunable Boron Nitride Nanotubes Combining Atomic Layer Deposition and Annealing Processes for Water Purification." Advanced Materials Interfaces, **5** (2018) 1800056.

[9] S. Iijima, "Helical microtubules of graphitic carbon." Nature, **354** (1991) 56.

[10] A. M. Marconnet et al., "Thermal conduction phenomena in carbon nanotubes and related nanostructured materials." Reviews of Modern Physics, **85** (2013) 1296.

[11] J.X. Zhao and B. Q. Dai, "DFT studies of electro-conductivity of carbon-doped boron nitride nanotube." Materials Chemistry and Physics, **88** (2004) 244.

[12] A. Rubio et al., "Theory of graphitic boron nitride nanotubes." Physical Review B, **49** (1994) 5081.

[13] N. G. Chopra et al., "Boron nitride nanotubes." Science, **269** (1995) 966-967.

[14] H. J. Xiang et al., "First-principles study of small-radius single walled BN nanotubes." Phys. Rev. B, **68** (2003) 035427.

[15] X. Chen et al., "Mechanical strength of boron nitride nanotube-polymer interfaces." Applied Physics Letters, **107** (2015) 253105.

[16] C. W. Chang et al., "Isotope effect on the thermal conductivity of boron nitride nanotubes." Physical Review Letters, **97** (2006) 085901.

[17] Y. Huang et al., "Growth mechanism and properties of highly pure ultrafine boron nitride nanotubes with diameters of sub-10 nm." Nanotechnology, **22** (2011) 145602.

[18] C. Zhi et al., "Perfectly dissolved boron nitride nanotubes due to polymer wrapping." Journal of American Chemical Society, **127** (2005) 15996.

[19] S. A. Thibeault et al., "Nanomaterials for radiation shielding." MRS Bull. **40** (2015) 836.

[20] J.H. Kang et al., "Multifunctional Electroactive Nanocomposites Based on Piezoelectric Boron Nitride Nanotubes." ACS Nano, **9** (2015) 11942.

[21] C. Tang et al., "Fluorination and Electrical Conductivity of BN Nanotubes." Journal of American Chemical Society, **127** (2005) 6552.

[22] X. Bai et al., "Deformation-Driven Electrical Transport of Individual Boron Nitride Nanotubes." Nano Letters, **7** (2007) 632.

[23] X. Blasé et al., "Stability and band gap constancy of boron nitride nanotubes." Europhysics Letters, **8** (1994) 335.

[24] A. M. Yadollahi et al.,"Thermoelectric properties of two sided-closed single-walled boron nitride nanotubes (6, 3)." Indian Journal of Physics, **96** (2022) 3493.

[25] D. A. Papaconstantopoulos and M.J. Mehl, "The Slater–Koster tight-binding method: a computationally efficient and accurate approach." Journal of Physics: Condensed Matter, **15** (2003) R413.

[26] D. Porath et al., "Single electron tunneling and level spectroscopy of isolated C60 molecules." Journal of Applied Physics, **81** (1997) 2241.

[27] L. Song, "Large scale growth and characterization of atomic hexagonal boron nitride layers." Nano Letters, **10** (2010) 3209.

[28] A. M. Yadollahi et al., "Effect of impurity and temperature changes on the thermoelectric properties of the (6, 3) two sided-closed single-walled boron nitride nanotubes ((6, 3) TSC-SWBNNTs)." Journal of Theoretical and Applied Physics (JTAP) **16** (2022) 162230.

[29] J. Schneider et al., "Anders Blom and Kurt Stokbro, ATK-ForceField: a new generation molecular dynamics software package." Modelling Simul. Materials Science and Engineering, **25** (2017) 085007.

[30] P. Zhao et al., "Rectifying behavior in nitrogen-doped zigzag single-walled carbon nanotube junctions." Solid State Communications, **152** (2012) 2040.

[31] M. Wang et al., "Spin transport properties in Fe-doped graphene/hexagonal boron-nitride nanoribbons heterostructures" Physics Letters A, **383** (2019) 2217.

[32] T. Markussen et al., "Surface decorated silicon nanowires: a route to high-ZT thermoelectrics." Physical Review Letters, **103** (2009) 055502.

[33] C. Rui et al., "Transport properties of B/P doped graphene nanoribbon field-effect transistor." Materials Science in Semiconductance Processing, **130** (2021) 105826.

[34] H. Alama and S. Ramakrishnab, "A review on the enhancement of figure of merit from bulk to nano-thermoelectric materials." Nano Energy, **2** (2013) 190.

[35] T. M. Tritt," Thermoelectric Materials: Principles, Structure, Properties, and Applications." Elsevier, Encyclopedia of Materials: Science and Technology, **2** (2002) 1.

[36] T. Markussen et al., "Surface-Decorated Silicon Nanowires: A Route to High-ZT Thermoelectrics." Physical Review Letters, **103** (2009) 055502.

[37] M. R. Roknabadi et al, "Electronic and optical properties of pure and doped boron-nitride nano." Physica. B, **410** (2013) 212.

[38] R. Sadeghi et al., "Thermoelectric properties of zigzag single-walled Carbon nanotubes and zigzag single-walled Boron Nitride nanotubes (9, 0)." IJND **13 (3)** (2022) 311..